LETTERS
PUBLISHED ONLINE: 25 OCTOBER 2009 | DOI: 10.1038/NPHYS1427
nature physics

Bias-voltage dependence of perpendicular spin-transfer torque in asymmetric MgO-based magnetic tunnel junctions

Se-Chung Oh[1]★, Seung-Young Park[2]★, Aurélien Manchon[3]★†, Mairbek Chshiev[3], Jae-Ho Han[4], Hyun-Woo Lee[4], Jang-Eun Lee[1], Kyung-Tae Nam[1], Younghun Jo[2], Yo-Chan Kong[5], Bernard Dieny[3] and Kyung-Jin Lee[5]‡

Spin-transfer torque[1,2] (STT) allows the electrical control of magnetic states in nanostructures[3–5]. The STT in magnetic tunnel junctions (MTJs) is of particular importance owing to its potential for device applications[6,7]. It has been demonstrated[8–11] that the MTJ has a sizable perpendicular STT ($\tau_\perp$, field-like torque), which substantially affects STT-driven magnetization dynamics. In contrast to symmetric MTJs where the bias dependence of $\tau_\perp$ is quadratic[8–10,12,13], it is theoretically predicted that the symmetry breaking of the system causes an extra linear bias dependence[11]. Here, we report experimental results that are consistent with the predicted linear bias dependence in asymmetric MTJs. The linear contribution is quite significant and its sign changes from positive to negative as the asymmetry is modified. This result opens a way to design the bias dependence of the field-like term, which is useful for device applications by allowing, in particular, the suppression of the abnormal switching-back phenomena.

The STT is composed of two vector components (Fig. 1a): the in-plane torque ($\tau_\parallel$) and the perpendicular torque ($\tau_\perp$, also called 'field-like torque') normal to $\tau_\parallel$. Whereas $\tau_\perp$ in fully metallic nanopillars is negligible and has been ignored in the analysis of experimental data[14], $\tau_\perp$ in MgO-based MTJs can be $10 \sim 30\%$ of $\tau_\parallel$ (refs 8–10). Previous theoretical[12,13] and experimental[8–10] studies indicate that $\tau_\perp$ is a symmetric function of the voltage V at low voltages; $\tau_\perp = C_0 + \sum_{i=1}^{\infty} C_{2i} V^{2i}$ where the bias-independent contribution C_0 is also known as the interlayer exchange coupling[15,16]. A more recent theoretical study[11] indicates however that the symmetric bias dependence is expected only in symmetric MTJs and that extra antisymmetric components may appear ($\tau_\perp = C_0 + \sum_{i=1}^{\infty} C_i V^i$) in asymmetric MTJs where the free and reference layers are made of different materials.

Here, we examined the bias dependence of $\tau_\perp$ in asymmetric MTJs. We studied two types of asymmetric MgO-based MTJ of the composition (thickness in nanometres) 15PtMn/2.5$Co_{90}Fe_{10}$/0.8Ru/2$Co_{40}Fe_{40}B_{20}$/0.7MgO/Free (Fig. 1a: see the Methods section for sample details) with the free layer in MTJ1 (MTJ2) being 1.8$Co_{20}Fe_{60}B_{20}$ (2.3$Co_{49}Fe_{21}B_{30}$). Note that in both MTJs, the free-layer compositions are different from the reference-layer composition. The tunnel magnetoresistance (TMR) of MTJ1 (MTJ2) is 175%/117% (195%/123%) at 4.2 K/300 K (Fig. 1b). Owing to the asymmetry in the MTJs, the current–voltage characteristics are not symmetric even in the parallel magnetic configuration (P state) (Fig. 1c). Note that $(d^2I/dV^2)_P$ at $V = 0$ has opposite sign for the MTJ1 and MTJ2, reflecting the different asymmetries in the two MTJs.

To determine the bias dependence of $\tau_\perp$, we used the thermal activation model[17,18],

$$t^{\pm} = f_0^{-1} \exp\left(\frac{E_B^{\pm}(1 \mp V/|V_C^{\pm}|)}{k_B T^*}\right) \quad (1)$$

where the upper (lower) signs apply to the antiparallel-to-parallel (parallel-to-antiparallel) switching, $t^{\pm}$ is the relaxation time, f_0 is the attempt frequency ($= 10^9\ s^{-1}$), k_B is the Boltzmann constant, T^* is the junction temperature taking into account the bias-induced heating and $V_C^{\pm}$ is the critical voltage for magnetization switching at $T^* = 0$ K. Here, the factor $(1 \mp V/|V_C^{\pm}|)$ arises from the voltage dependence of the energy barrier due to the in-plane torque $\tau_\parallel$. The junction temperature T^* is obtained from commonly used estimation methods (see the Methods section and Supplementary Note S1). Here, $E_B^{\pm}$ reads

$$E_B^{\pm} = E_B^0 \left(1 \pm \frac{H_{ext} - H_{sh} + b_J}{H_C^{0\,K}}\right)^n \quad (2)$$

where E_B^0 is the intrinsic energy barrier, H_{ext} is the external magnetic field applied along the easy axis, H_{sh} is the shift field owing to the orange-peel coupling[19] as well as the interlayer exchange coupling C_0, $H_C^{0\,K}$ is the coercivity at $T^* = 0$ K and n ($= 3/2$; refs 20, 21) is the exponent characterizing the field-dependence of the energy barrier. Here, we introduce b_J to describe the bias-induced field-like effect, and use the lowest-order expansion $b_J = C_1 V + C_2 V^2$ to capture the main effects of its asymmetric and symmetric bias-dependent components. Effects of C_1 and C_2 on $E_B^{\pm}$ are illustrated in Fig. 2a. At this stage, we do not identify b_J with the bias-dependent part of $\tau_\perp$ because such a field-like effect in the thermally activated switching may involve a number of mechanisms: $\tau_\perp$, non-macrospin processes or bias-induced heating. Below, we

[1]Semiconductor R&D Center, Samsung Electronics Co, Gyeonggi-Do 445-701, Korea, [2]Nano Material Research Team, Korea Basic Science Institute, Daejeon 305-333, Korea, [3]SPINTEC, UMR 8191 CEA/CNRS/UJF, CEA/Grenoble, 38054 Grenoble cedex 9, France, [4]PCTP and Department of Physics, Pohang University of Science and Technology, Pohang, Kyungbuk 790-784, Korea, [5]Department of Materials Science and Engineering, Korea University, Seoul 136-713, Korea. *These authors contributed equally to this work. †Present address: Department of Materials Science and Engineering, King Abdullah University of Science and Technology, Thuwal 23955-6900, Saudi Arabia. ‡e-mail: kj_lee@korea.ac.kr.

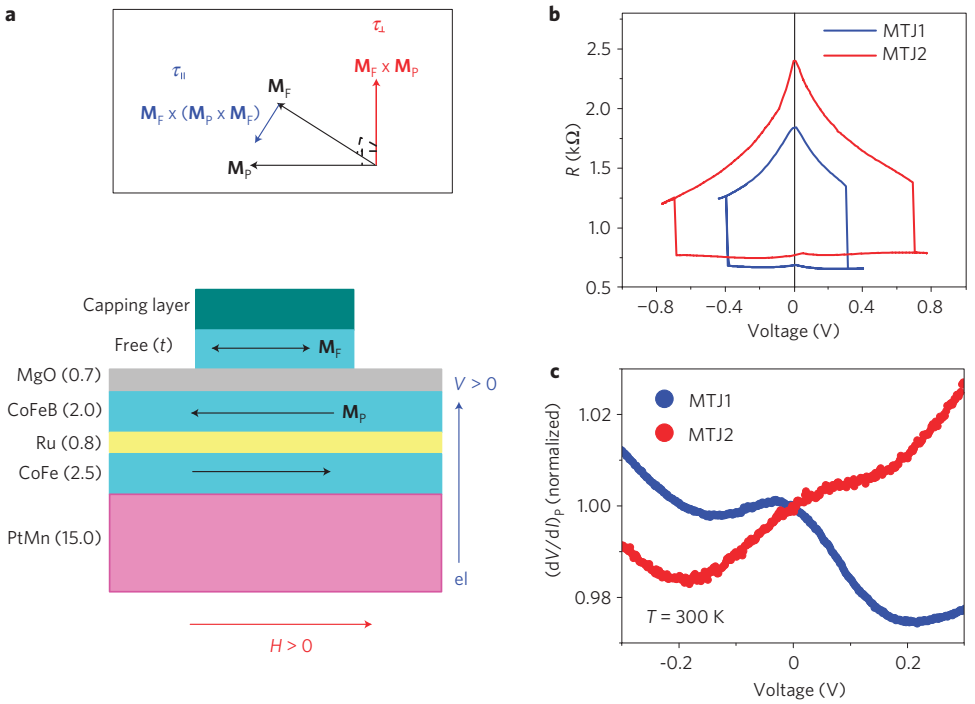

Figure 1 | Magnetoresistive properties of asymmetric MgO-based MTJs. a, Schematic of MTJ layer structure (all in nanometres). $\mathbf{M}_F$ ($\mathbf{M}_P$) is the free- (reference)-layer magnetization vector. Positive bias corresponds to electrons flowing from the reference layer to the free layer and thus favours parallel alignment of the two layers. Positive external field favours the antiparallel alignment. The top panel shows the two components $\tau_\parallel$ and $\tau_\perp$ of the STT acting on $\mathbf{M}_F$. **b**, Resistance versus bias voltage for MTJ1 and MTJ2 measured at $T = 4.2$ K. **c**, Room-temperature (dV/dI) versus voltage curves in the P state.

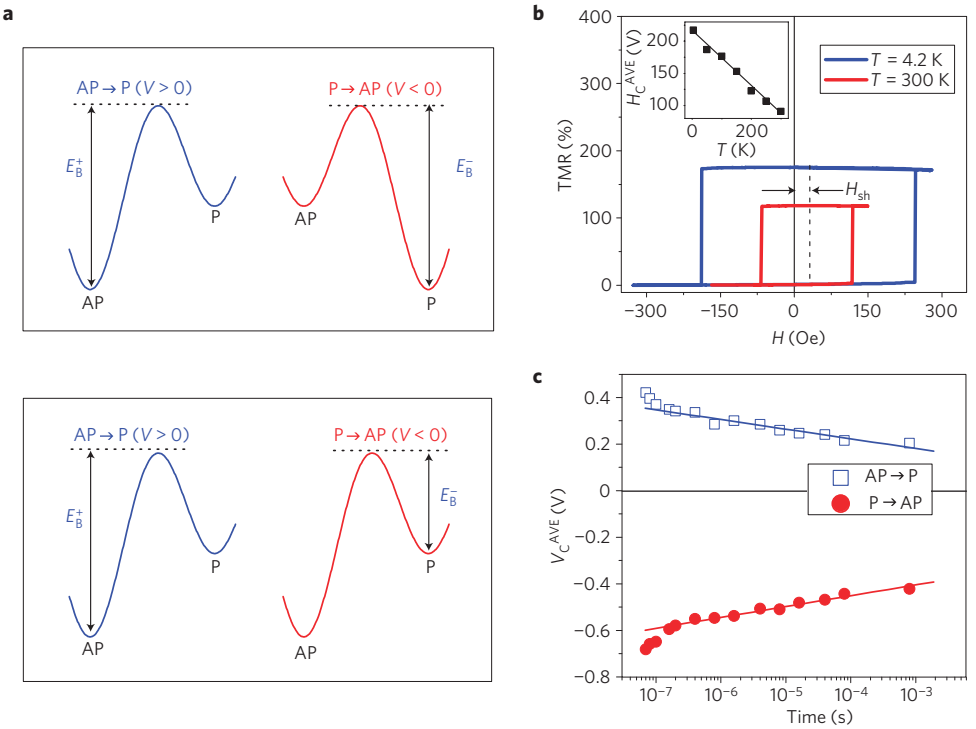

Figure 2 | Temperature-dependent switching field H_C and pulse-width-dependent switching voltage V_C (MTJ1). a, Schematic of the effect of b_J on $E_B^\pm$ in the two limiting cases; b_J possesses only antisymmetric components (for instance, $b_J = C_1 V$; see top panel) and only symmetric components (for instance, $b_J = C_2 V^2$; see bottom panel). If $b_J = C_1 V$, E_B^+ and E_B^- are expected to be the same, as b_J changes sign when changing the voltage polarity. The sign of C_1 determines whether or not $E_B^\pm > E_B^0$. In contrast, if $b_J = C_2 V^2$, E_B^+ is different from E_B^- because b_J keeps its sign regardless of the voltage polarity. The sign of C_2 determines whether or not $E_B^+ > E_B^-$. **b**, TMR versus the external field measured at $T = 4.2$ and 300 K. H_{sh} is the shift field originating from the orange-peel coupling and C_0. In our samples, the orange-peel coupling seems to be dominant over C_0 because C_0 generates a negative H_{sh} for a tunnelling barrier thickness below 1 nm (ref. 16), whereas the observed H_{sh} is positive. Inset: Temperature-dependent H_C. **c**, V_C versus log-scaled pulse width at $T = 300$ K. The lines are linear fits for pulse-width > 500 ns. In **c** and the inset of **b**, V_C and H_C are averaged values from five measurements.

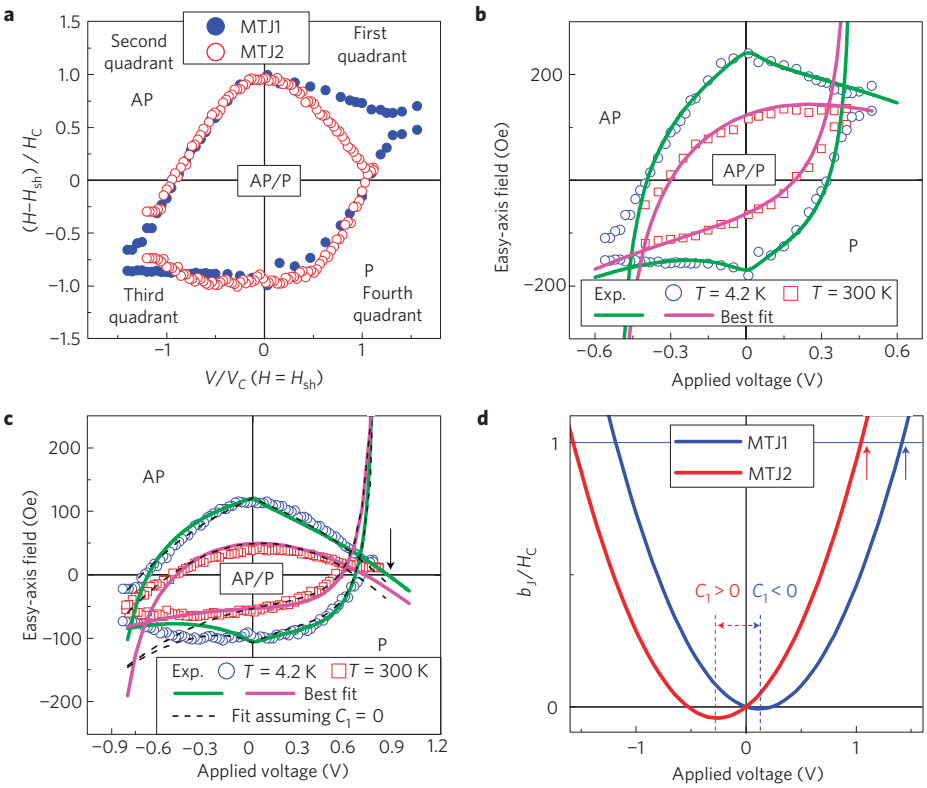

Figure 3 | Switching phase diagram of MTJ1 and MTJ2. a, Normalized switching phase diagram of two MTJs measured at $T = 4.2$ K. **b**, Switching phase diagram of MTJ1 measured at $T = 4.2$ and 300 K. The lines are the best fits using the thermal activation model. The best fit is obtained for experimentally measured parameters ($E_B^0/(k_B(300\,K)) = 61$, $H_C^{4.2\,K} = 218$ Oe and $H_{sh} = 30$ Oe) and fitting parameters ($C_1 = -30\,Oe\,V^{-1}$, $C_2 = +130\,Oe\,V^{-2}$, $V_C^+ = 0.44$ V, $V_C^- = -0.56$ V, $\gamma_{APtoP} = 3.2 \times 10^{11}\,K^2\,A^{-2}$ and $\gamma_{PtoAP} = 1.3 \times 10^{11}\,K^2\,A^{-2}$). **c**, Switching phase diagram of MTJ2. The best fit is obtained for experimentally measured parameters ($E_B^0/(k_B(300\,K)) = 62$, $H_C^{4.2\,K} = 118$ Oe and $H_{sh} = 10$ Oe) and fitting parameters ($C_1 = +38\,Oe\,V^{-1}$, $C_2 = +72\,Oe\,V^{-2}$, $V_C^+ = 0.82$ V, $V_C^- = -0.93$ V, $\gamma_{APtoP} = 2.3 \times 10^{11}\,K^2\,A^{-2}$ and $\gamma_{PtoAP} = 0.7 \times 10^{11}\,K^2\,A^{-2}$). The dashed lines in **c** are fits assuming $C_1 = 0$ ($C_2 = +120\,Oe\,V^{-2}$, $V_C^+ = 0.82$ V, $V_C^- = -2.70$ V, $\gamma_{APtoP} = 2.3 \times 10^{11}\,K^2\,A^{-2}$ and $\gamma_{PtoAP} = 0.7 \times 10^{11}\,K^2\,A^{-2}$). Note that an unrealistically large V_C^- has to be used for this fit. **d**, Normalized b_J obtained from the best fit as a function of the voltage.

first evaluate b_J and then discuss its relationship with $\tau_\perp$. From equations (1) and (2), one derives the switching threshold voltage V_C (or switching threshold field H_C) from $\exp(-t/t^\pm) = 1/2$ for the observation time t. The comparison between the calculated switching thresholds and experimentally measured values allows the evaluation of unknown parameters.

We first determined E_B^0 from the temperature-dependent H_C at $V \sim 0$ V (Fig. 2b, inset) and found $E_B^0/(k_B(300\,K)) = 61$ for MTJ1. Another approach widely used in the literature[6,7] consists of estimating $E_B^\pm$ from the relationship between the critical voltage V_C and the pulse width t of the voltage bias (Fig. 2c). However, this approach should be used cautiously. In the literature[6,7], the role of b_J in $E_B^\pm$ and the bias-induced heating are commonly ignored. If this common practice were correct, it should yield the same value for $E_B^\pm$ as E_B^0 (= 61 for MTJ1). Within these approximations, we found however that the experimental estimations of $E_B^\pm$ strongly differ from E_B^0: $E_B^+/(k_B(300\,K)) = 37$ for $V > 0$ and $E_B^-/(k_B(300\,K)) = 25$ for $V < 0$, indicating that effects of b_J and of heating should be considered as in the following analysis.

To evaluate b_J, we used the switching phase diagrams (SPDs) where H_C is measured as a function of V at 4.2 and 300 K. Figure 3a shows the normalized SPDs at 4.2 K for the two MTJs. In the second quadrant ($H_{ext} > 0$ and $V < 0$), both H_{ext} and $\tau_\parallel$ favour the parallel-to-antiparallel switching, whereas in the fourth quadrant ($H_{ext} < 0$ and $V > 0$), both favour the antiparallel-to-parallel switching. Under these bias conditions, b_J has only a minor role and the normalized phase boundaries are almost identical for both MTJs. In contrast, H_{ext} and $\tau_\parallel$ compete with each other in the first and third quadrants. Correlatively, b_J has a strong influence in these quadrants. The difference between MTJ1 and MTJ2 in the first and third quadrants (Fig. 3a) implies different bias dependence of b_J in the two MTJs.

For the MTJ1 SPD at 4.2 K, the best fitting is obtained with $C_1 = -30\,Oe\,V^{-1}$ and $C_2 = +130\,Oe\,V^{-2}$ (Fig. 3b). These parameters also fit the SPD at 300 K reasonably well, indicating that the temperature dependence of C_1 and C_2 is not strong (see Supplementary Note S1). We also measured the MTJ2 SPDs and obtained the best fittings with $C_1 = +38\,Oe\,V^{-1}$ and $C_2 = +72\,Oe\,V^{-2}$ (Fig. 3c). We point out that if C_1 is assumed to be zero, no satisfactory fits of the SPD boundaries in all four quadrants can be obtained (see Fig. 3c and its caption). Thus, considering a non-zero C_1 is essential to properly describe the switching boundaries. In Supplementary Note S2, we check the applicability of the fitting parameters to the situation with an in-plane hard-axis field. We also point out that the sign of C_1 is different for MTJ1 and MTJ2 (Fig. 3d).

To clarify the relationship between b_J and $\tau_\perp$, we discuss possible mechanisms, other than $\tau_\perp$, that may contribute to b_J. Field-like effects may arise from non-macrospin processes, which can become important when $\tau_\parallel$ acts as an anti-damping term[14]. However, in the first and third quadrants, $\tau_\parallel$ acts as a damping term and therefore contributes to suppress non-macrospin processes. Thus, the development of magnetic inhomogeneities cannot explain the significant difference between the two MTJs' SPDs in the first and third quadrants (Fig. 3a).

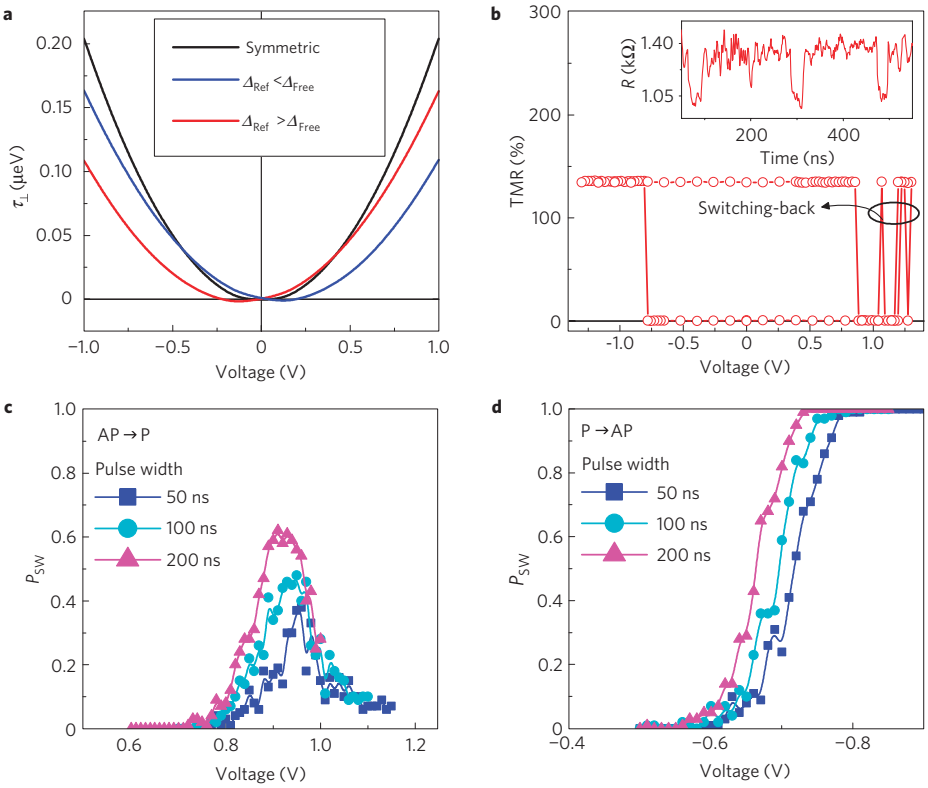

Figure 4 | Sign of C_1 and abnormal switching-back phenomenon. a, Theoretical result of bias-dependent $\tau_\perp$ for asymmetric Δ (see the Methods section for details of parameters). **b**, Experimental results of TMR versus voltage measured at pulse width = 50 ns, $H_{ext} = 0$ and $T = 300$ K for MTJ2. The switching-back is observed when $V > +1.0$ V. Inset: Random telegraphic noise measured at $V = +1.0$ V and $H_{ext} = 0$ Oe. **c**,**d**, Zero-field switching probability P_{SW} at various voltages and pulse widths for MTJ2. **c** is for positive voltages, whereas **d** is for negative voltages.

Inaccuracies in the estimation of the junction temperature T^* may lead to a twisted evaluation of C_i values. As T^* is also bias dependent, the evaluation of C_i values depends fundamentally on the estimation of $T^*(V)$. To gain insight into this issue, we examined several heating estimation methods commonly used for MTJs (refs 18, 22) and found about 10% variation of C_i values (see Supplementary Note S1), which is not a crucial correction. This estimation is also supported by the observation that in the first and third quadrants, which are most influential for the evaluation of C_i values, the effective energy barrier $E_B^{\pm}(1 \mp V/|V_C^{\pm}|)$ is larger and thus the bias-induced heating is less important than in the second and fourth quadrants.

The reliability of the above estimation depends on how realistic the assumed forms of $T^*(V)$ are. Whereas all forms of $T^*(V)$ used in our analysis assume a quadratic bias dependence, a linear dependence may arise owing to thermoelectric effects, related to the Peltier effect in metallic spin-valves[23] or tunnelling of electrons through normal metal–insulator–superconductor junctions[24]. However, these mechanisms could be important only when the two electrodes are made of considerably different materials[24,25], and thus do not seem relevant to the present situation (that is, the same atomic elements with different compositions). On the basis of this discussion, we conclude that $\tau_\perp$ is most likely responsible for the observed b_J. At this point, we also mention that for a more quantitative evaluation of $\tau_\perp$, an accurate experimental estimation of T^* is crucial, which is a subject of future studies.

Next we discuss possible origins of the non-zero C_1 and its sign change in the context of $\tau_\perp$. Previous studies on symmetric MTJs suggested[10,18] that at high bias, the bias dependence of $\tau_\perp$ can become asymmetric owing to hot electron-related magnon excitations. However, this mechanism allows only one sign of C_1 and thus is inconsistent with our observation of the sign change of C_1. A thickness difference between the free and reference layers can also result in non-zero C_1 (ref. 26). This mechanism is however suppressed in the presence of thickness fluctuations as small as a single atomic layer[13], responsible for the finite orange-peel coupling in our samples. Still another possible mechanism is the asymmetry in the exchange splitting Δ. A recent theoretical study[11] demonstrated that the asymmetric bias dependence of $\tau_\perp$ can be either positive or negative depending on the relative magnitudes of Δ in the reference and free layers (Δ_{Ref} and Δ_{Free}). Note that in MTJ1 (MTJ2), the free layer is Fe-rich (Co-rich), whereas the atomic concentrations of Fe and Co are the same in the reference layer. Therefore, in MTJ1 (MTJ2), Δ_{Free} is expected to be larger (smaller) than Δ_{Ref} because Fe has a larger Δ than Co (ref. 27).

To investigate the relationship between the asymmetric Δ and the sign of C_1, we carried out a model calculation of the bias-dependent $\tau_\perp$ using the free-electron model within the Keldysh formalism[26] (see the Methods section for model parameters). We found that C_1 is negative (positive) when $\Delta_{Ref} < (>) \Delta_{Free}$ (Fig. 4a). Therefore, the effect of an asymmetric Δ on $\tau_\perp$ is qualitatively consistent with the experimental observations. We also tested another possible source of the symmetry breaking, that is, asymmetric barrier height U because the workfunctions of Co, Fe and B are different[28]. We found however that this effect generates incorrect C_1 signs (see Supplementary Note S3).

The voltage dependence of b_J affects an abnormal switching behaviour at large voltage, which is expected to have significant implications in MTJ-based devices. As indicated by solid up-arrows in Fig. 3d, b_J becomes larger than H_C when V increases above a certain threshold. Under these conditions, the influence of b_J and $\tau_\parallel$ starts competing: $\tau_\parallel$ favours the parallel (antiparallel) state for a positive (negative) V, whereas b_J favours the antiparallel state regardless of the voltage polarity. Consequently, when V is positively

large, an abnormal switching-back phenomenon is observed, where the parallel-to-antiparallel and antiparallel-to-parallel switchings coexist and thus the random telegraphic noise is observed at $H_{ext} = 0$ (MTJ2: Fig. 4b and inset). The critical voltage for the switching-back is about +1.0 V (+1.4 V) for MTJ2 (MTJ1), corresponding to the voltage at which the phase boundary crosses the zero field axis (indicated by a down-arrow in Fig. 3c). For a better understanding, the switching probability P_{SW} from 100 switching trials was measured at various voltages and pulse widths for MTJ2. For $V > +1.0$ V, P_{SW} abnormally decreases with increasing V (Fig. 4c), whereas for $V < 0$, P_{SW} shows a normal behaviour (Fig. 4d).

An important aspect of the observed switching-back phenomenon is that it can be controlled by material engineering of ferromagnetic electrodes, thus allowing a tuning of C_1. In MTJ2, the positive C_1 decreases the switching-back threshold down to +1.0 V, whereas in MTJ1, the negative C_1 increases the threshold up to +1.4 V above the breakdown voltage so that no switching-back is observed. Recent experimental studies[29,30] reported switching-back phenomena at both voltage polarities. The authors ascribed this observation to a reduced anisotropy field at elevated bias. Note that, in our case, the switching-back is observed at only one polarity, which requires a strong asymmetry in thermally activated switching as discussed above.

Methods

Sample preparation. The resistance–area product for the parallel configuration in our MTJs is about 7–9 $\Omega\,\mu m^2$. The top CoFeB layer was patterned by photolithography and the reactive-ion etching technique to produce an elliptical cross-section with a nominal size of $180 \times 80\ nm^2$. The etching was stopped at the MgO barrier and thus the bottom layer is unpatterned to minimize the stray field originating from the bottom ferromagnetic electrode. After the patterning process, MTJs were annealed at 300 °C for 2 h under an easy-axis magnetic field of 1 T to enhance the TMR and exchange bias. Measurements were carried out on five samples of each type and show similar results. The data presented in this letter are from one sample for each type of MTJ.

Bias-induced heating. To account for bias-induced heating in the thermal activation model (equations (1) and (2)), we used the following formula for junction temperature: $T^* = \sqrt{T^2 + \gamma_{APtoP} I^2}$ ($T^* = \sqrt{T^2 + \gamma_{PtoAP} I^2}$) when the system is initially in the antiparallel (parallel) configuration[22]. Here, T is the ambient temperature (4.2 or 300 K), I ($= V/[R(V, T, P/AP)]$) is the current, $R(V, T, P/AP)$ is the experimentally determined junction resistance and γ_{APtoP} and γ_{PtoAP} are parameters that depend on the material and geometric heat-transport characteristics. We also tested other heating models[18] and found that all of these heating models give similar fitting values of C_1 and C_2 within 10% difference (see Supplementary Note S1).

Parameters used in the theoretical model for calculating the spin torques. Details of the model are described in ref. 26. The MTJ consists of two semi-infinite ferromagnets separated by a 0.7-nm-thick insulator with an effective mass $m_e^* = 0.4 m_e$. For the symmetric MTJ, the barrier height U is 3 eV and the exchange splitting Δ is 1 eV. For the asymmetric MTJs, U is kept at a constant of 3 eV, whereas Δ of one ferromagnet is 1.6 eV and Δ of the other ferromagnet is 0.4 eV.

Received 11 May 2009; accepted 4 September 2009; published online 25 October 2009

References

1. Slonczewski, J. C. Current-driven excitation of magnetic multilayers. *J. Magn. Magn. Mater.* **159,** L1–L7 (1996).
2. Berger, L. Emission of spin waves by a magnetic multilayer traversed by a current. *Phys. Rev. B* **54,** 9353–9358 (1996).
3. Myers, E. B., Ralph, D. C., Katine, J. A., Louie, R. N. & Buhrman, R. A. Current-induced switching of domains in magnetic multilayer devices. *Science* **285,** 867–870 (1999).
4. Kiselev, S. I. *et al.* Microwave oscillations of a nanomagnet driven by a spin-polarized current. *Nature* **425,** 380–382 (2003).
5. Yamaguchi, A. *et al.* Real-space observation of current-driven domain wall motion in submicron magnetic wires. *Phys. Rev. Lett* **92,** 077205 (2004).
6. Ikeda, S. *et al.* Magnetic tunnel junctions for spintronic memories and beyond. *IEEE Trans. Electron Devices* **54,** 991–1002 (2007).
7. Diao, Z. *et al.* Spin transfer switching in dual MgO magnetic tunnel junctions. *Appl. Phys. Lett.* **90,** 132508 (2007).
8. Sankey, J. C. *et al.* Measurements of the spin-transfer-torque vector in magnetic tunnel junctions. *Nature Phys.* **4,** 67–71 (2008).
9. Kubota, H. *et al.* Quantitative measurement of voltage dependence of spin-transfer torque in MgO-based magnetic tunnel junctions. *Nature Phys.* **4,** 37–41 (2008).
10. Deac, A. M. *et al.* Bias-driven high-power microwave emission from MgO-based tunnel magnetoresistance devices. *Nature Phys.* **4,** 803–809 (2008).
11. Xiao, J., Bauer, G. E. W. & Brataas, A. Spin-transfer torque in magnetic tunnel junction: Scattering theory. *Phys. Rev. B* **77,** 224419 (2008).
12. Theodonis, I., Kioussis, N., Kalitsov, A., Chshiev, M. & Butler, W. H. Anomalous bias dependence of spin torque in magnetic tunnel junctions. *Phys. Rev. Lett.* **97,** 237205 (2006).
13. Heiliger, C. & Stiles, M. D. *Ab initio* studies of the spin-transfer torque in magnetic tunnel junctions. *Phys. Rev. Lett.* **100,** 186805 (2008).
14. Lee, K. J., Deac, A., Redon, O., Nozières, J. P. & Dieny, B. Excitations of incoherent spin-waves due to spin-transfer torque. *Nature Mater.* **3,** 877–881 (2004).
15. Slonczewski, J. C. Conductance and exchange coupling of two ferromagnets separated by a tunneling barrier. *Phys. Rev. B* **39,** 6995–7002 (1989).
16. Faure-Vincent, J. *et al.* Interlayer magnetic coupling interactions of two ferromagnetic layers by spin polarized tunneling. *Phys. Rev. Lett.* **89,** 107206 (2002).
17. Li, Z. & Zhang, S. Thermally assisted magnetization reversal in the presence of a spin-transfer torque. *Phys. Rev. B* **69,** 134416 (2004).
18. Li, Z. *et al.* Perpendicular spin torques in magnetic tunnel junctions. *Phys. Rev. Lett.* **100,** 246602 (2008).
19. Néel, L. Magnetisme—sur un nouveau mode de couplage entre les aimantations de deux couches minces ferromagnetiques. *Comptes Rendus Acad. Sci.* **255,** 1676–1681 (1962).
20. Victora, R. H. Predicted time dependence of the switching field for magnetization. *Phys. Rev. Lett.* **63,** 457–460 (1989).
21. Krivorotov, I. N. *et al.* Temperature dependence of spin-transfer-induced switching of nanomagnets. *Phys. Rev. Lett.* **93,** 166603 (2004).
22. Fuchs, G. D. *et al.* Adjustable spin torque in magnetic tunnel junctions with two fixed layers. *Appl. Phys. Lett.* **86,** 152509 (2005).
23. Hatami, M. *et al.* Thermoelectric effects in magnetic nanostructures. *Phys. Rev. B* **79,** 174426 (2009).
24. Clark, A. M. *et al.* Cooling of bulk material by electron tunneling refrigerators. *Appl. Phys. Lett.* **86,** 173508 (2005).
25. Fukushima, A., Kubota, H., Yamamoto, A., Suzuki, Y. & Yuasa, S. Peltier effect in metallic junctions with CPP structures. *IEEE Trans. Magn.* **41,** 2571–2573 (2005).
26. Manchon, A., Ryzhanova, N., Vedyayev, A., Chschiev, M. & Dieny, B. Description of current-driven torques in magnetic tunnel junctions. *J. Phys. Condens. Matter.* **20,** 145208 (2008).
27. Eastman, D. E., Himpsel, F. J. & Knapp, J. A. Experimental exchange-split energy-band dispersions for Fe, Co and Ni. *Phys. Rev. Lett.* **44,** 95–98 (1980).
28. Michaelson, H. B. The work function of the elements and its periodicity. *J. Appl. Phys.* **48,** 4729–4733 (1977).
29. Sun, J. Z. *et al.* High-bias backhopping in nanosecond time-domain spin-torque switches of MgO-based magnetic tunnel junctions. *J. Appl. Phys.* **105,** 07D109 (2009).
30. Min, T., Sun, J. Z., Beach, R., Tang, D. & Wang, P. Back-hopping after spin torque transfer induced magnetization switching in magnetic tunneling junction cells. *J. Appl. Phys.* **105,** 07D126 (2009).

Acknowledgements

We acknowledge S. Zhang, B. C. Min, C.-Y. You and G. E. W. Bauer for discussions and M. H. Jung for measurement set-up. This work was supported by the Korea Science and Engineering Foundation (KOSEF) through the National Research Laboratory program (Project No. M10600000198-06J0000-19810) (for K.-J.L.), the Basic Research Program (Contract No. R01-2007-000-20281-0) (for H.-W.L.) funded by the Korean Ministry of Science and Technology and by grant No. KSC-2008-S01-0012 from Korea Institute of Science and Technology Information (for K.-J.L.), the KBSI grant T29513 (for Y.J.), NSF (Contract No. DMR-0704182) (for A.M.), University of Alabama through Adjunct Professorship (for M.C.) and Chair of Excellence Research Program of the Nanosciences Foundation (RTRA) in Grenoble, France (for M.C.).

Author contributions

S.-C.O., A.M., B.D. and K.-J.L. initiated and designed the experiments. S.-C.O., J.-E.L. and K.-T.N. fabricated the samples and carried out the pulse measurements for the switching-back. S.-Y.P. and Y.J. carried out all other measurements. A.M., M.C., J.-H.H., H.-W.L., Y.-C.K. and K.-J.L. developed the theoretical models and interpreted the data. K.-J.L. prepared the manuscript with help from B.D., A.M. and H.-W.L. All authors discussed the result and commented on the manuscript.

Additional information

Supplementary information accompanies this paper on www.nature.com/naturephysics. Reprints and permissions information is available online at http://npg.nature.com/reprintsandpermissions. Correspondence and requests for materials should be addressed to K.-J.L.